Structural and optical properties of Zn doped $CuInS_2$ thin films

MAHDI H.SUHAIL
Dept. of Physics, College of Science, Univ. of Baghdad-Iraq

Copper indium sulphide (CIS) films were deposited by spray pyrolysis onto glass substrates from aqueous solutions of copper (II) sulphate, indium chloride and thiourea using compressed air as the carrier gas. The copper/indium molar ratio (Cu/In) in the solution 1(1:1) and the sulphur/copper ratio (S/Cu) was fixed at 4.The structural properties of these films were characterized. The effects of Zn [(0%–5%) molecular weight compared with $CuInS_2$ Source] and different substrate temperatures on films properties were investigated using X-ray diffraction (XRD) and optical transmission Spectra. Optical characteristics of the $CuInS_2$ films have been analyzed using spectrophotometer in the wavelength range of 300–1100 nm. The absorption spectra of the films showed that this compound is a direct band gap material and gap values varied between 1.55–1.57 eV, depending on the substrate temperatures. The Zn-doped samples have band gap energy of 1.55-1.95 eV. It was observed that there is an increase in optical band gap with increasing Zn % molecular weight. The optical constants of the deposited films were obtained from the analysis of the experimental recorded transmission and absorption Spectral data The refractive index n and dielectric constants ε_1 and ε_2 were also discussed and calculated as a function of investigated wavelength range and found it dependent on Zn incorporation. We found that the Zn-doped $CuInS_2$ thin films exhibit P-type conductivity and we predict that Zn species can be considered as suitable candidates for use as doped acceptors to fabricate $CuInS_2$-based solar cells. The paper presents a study concerning the influence of deposition parameters (temperature of the substrate and concentration of Zn (1-5)% from 0.16 M $ZnCl_2$) on the quality of $CuInS_2$ thin films achieved by spray pyrolysis on glass substrate from solutions containing0.02 M $CuCl_2 \cdot 2H_2O$, 0.16 M thiourea and 0.08 M $In_2Cl_3.5H_2O$.

(Received January 10, 2012; accepted February 20, 2012)

Keywords: $CuInS_2$, Doping, Structural properties, Optical properties, Copper compounds, Ternary semiconductors, Semiconductor epitaxial layers, Thin films solar cell, Optical constants

1. Introduction

The chemical spray pyrolysis (CSP) technique offers an extremely easy way to prepare films with dopants, virtually any element in any proportion by merely adding it in a spray solution. The deposition rate and thickness of the film can easily be controlled for a wide range. It also offers an opportunity to have reactions at low temperatures (100-500^{0}C). These methods can also produce films on substrates that are less robust materials and on large surfaces. The versatile nature of this technique lies in the way various parameters that include effect of precursors, dopants, substrates temperature, in-situ annealing treatments, solution concentrations and so on can easily be controlled. Various types of metal oxide, metallic spinel oxide, binary and ternary chalcogenides and superconducting oxides can be prepared [1].

Ternary chalcopyrite $CuInS_2$ thin films exhibit many excellent physical and chemical properties such as high absorption coefficient in the visible spectral range [2], high tolerance to the presence of defects [3], an direct band gap closes to 1.5 eV, the optimum value for the photovoltaic conversion of solar energy [4], possibility to avoid n- and p-type conductivity [5] and high chemical stability. In contrast to other ternary semiconductor materials, $CuInS_2$ is nontoxic, low-cost and easy to fabricate by various thin film deposition techniques [6-8]. For controlling a conduction type and obtaining low resistivity, several impurities doped $CuInS_2$ bulks have been studied. Akaki et al [9] studied the structural, electrical and optical properties of Bi-$CuInS_2$ thin films grown by vacuum evaporation method. Zribi et al [10] investigated the effect of Na doping on the properties of $CuInS_2$ thin films and obtained more interesting results. The incorporation of Fe during the crystal growth of $CuInS_2$ by chemical vapor transport was studied [10], [11] and the results of electrical and photoluminescence measurements of P-doped and Zn-doped $CuInS_2$ crystals were reported. Yamamoto et al [12],[13] investigated the electronic structures of n-type doped $CuInS_2$ crystals using Zn and Cd species and showed that *p*-type doping using the group V elements such as N, P and As increases the Madelung energy, which gives rise to instability of ionic charge distribution in *p*-type doped $CuInS_2$ crystals [14]. Enzenhofer et al [15] showed that the open circuit voltage of solar cells based on $CuInS_2$ can be enhanced via controlled doping of small amounts of Zinc.

In this paper, we report on structural and optical properties of the Zn-doped $CuInS_2$ thin films as a function of substrate temperatures and Zn concentration.

2. Experimental

The spray pyrolysis technique is a simple technology in which an ionic solution -containing the constituent elements of a compound in the form of soluble salts- is sprayed onto over heated substrates using a stream of clean, dry air. The $CuInS_2$ thin films were prepared by spraying an aqueous solution of In_2Cl_3, $CuCl_2$ and thiourea $[(NH_2)_2CS]$ on glass substrate kept at 250, 300 and 350° C.

The atomization of the chemical solution into a spray of fine droplets is effected by the spray nozzle, with the help of compressed air as carrier gas. The spray rate was about 15 cm^3/min through the nozzle ensures a uniform film thickness. The apparatus used to carry out the chemical spray process consists basically of a device used to atomize the spray solution and some sort of substrate heater. Our setup consists of a reaction chamber foreseen to its lower part with a plate heated by electrical resistance. Standard commercial glass slides (25×25×1 mm^3) were used as substrates, which were previously cleaned well using detergent, water and dried prior to the film deposition process.

Substrate temperature is measured with a thermocouple. Above the substrate at variable distances (10 - 50 cm) the glass-spraying nozzle is fixed. The solution is sprayed (from a reservoir) by means of the carrier gas, incidently to the substrate. The gas (dry air used as a carrier gas) flow rate was 13 ml/min. The spraying time vary between 10 - 20 seconds for one layer, and the layer number between 1- 5. The heater is a cylindrical stainless steel block furnace electrically controlled to an accuracy of ± 2 ^{0}C. The substrate temperature was varied, while the other spray parameters were kept constant. The thickness of the film was 400 nm and established by micro weighting or spectrophotometrically as described in Ref [16] The X-ray diffraction (XRD) patterns of the films were recorded with a JEOL 60 PA X-ray diffractometer operating with a 0.15418 nm monochromatized Cu- K_α radiation at 40 kV and 30 mA with Ni filter. Transmission *T* & absorption A spectra of the prepared samples were measured by normal incidence of light using a double beam UV-3101 PC Scanning Shimadzu spectrophotometer, in the wavelength range 400-1000 nm, using a blank substrate as the reference position.

3. Results and discussion

3.1. Structure of the $CuInS_2$ thin films

Fig. 1 shows the X-ray diffraction patterns of undoped $CuInS_2$ thin films which are deposited on glass substrates at substrate temperatures 250. 300. 350°C and substrate temperature 350° C annealed in air to 200°C for 2.5 hours. No XRD peaks corresponding to any phase of crystalline CIS were found when the films were sprayed onto substrates at temperatures lower than 250 °C. The XRD spectra reveal that all obtained films sprayed at substrate temperatures equal to 250 °C or higher are polycrystalline with chalcopyrite structure (JCPDS File No. 047–1372) with a preferred orientation at 2θ =27.9° assigned to the (112) reflection of $CuInS_2$ phase. CIS films prepared show a chalcopyrite structure with present significant differences in their crystalline structure for both temperatures and temperature annealed to 200 °C for 2.5 h.

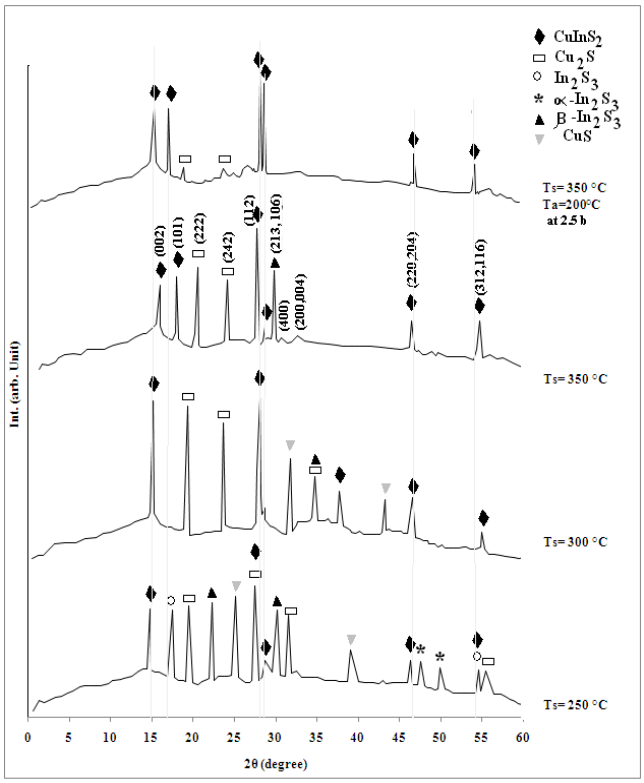

Fig.1. Shows the X-ray diffraction patterns of the $CuInS_2$ films at different substrate temperatures

The grain size along the (112) peak can be evaluated by using the Debye Scherrer relation [17]:

$$L = 0{:}9\,\lambda / \cos(\theta_0)\,\Delta(2\theta);$$

Where 2θ is the half intensity width of the peak and θ_0 the Bragg angle.

The FWHM values of the (112) diffraction peak decrease when the substrate temperature rises from 250 to 350 °C indicating that the crystallite size is bigger for films sprayed at 350 °C. The increase in grain size due to recrystall-ization processes.

Although this phenomenon was observed in several samples sprayed under the same conditions, this work focuses on the conditions that make possible the synthesis of crystalline CIS films.

We note also some additional diffraction peaks at different Bragg angle which can be associated to binary compounds In_2S_3, CuS and Cu_2S crystal and these phases was not investigated in detail. This result was agreed with Sahal etal [18].

It is clear, to state the important role of temperature in the films crystallization. The pattern for the film displayed diffraction peaks at 2θ values of approximately 16°, 16.75°, 20.73°, 23.42° and 31.63° which corresponding to (002), (101), (242) ,(200),(220) and (116) planes respectively . It may be noted that a secondary phase with peaks assigned to (222), (400) and (312) planes appears which attributed to the Cu_2S, CuS and In_2S_3 material. In addition, we note that an increase in substrate temperatures leads to an improvement in the crystallinity of the films [19],[20].

3.2. Structure of the $CuInS_2$thin films doped with Zinc

Fig. 2 shows the results of our XRD measurements of non-doped and doped $CuInS_2$ thin films with Zn concentration. It is found that the zinc concentration has great effects on the formation of polycrystalline $CuInS_2$. All diagrams present peak at 2θ = 27.9° assigned to the (112) reflection of $CuInS_2$ phase and there is an improvement in the growth for all the samples containing Zn. It is also observed that the intensity of the (112) peak decreases obviously with increasing zinc concentrations, which probably may be due to increase of the disorder component.

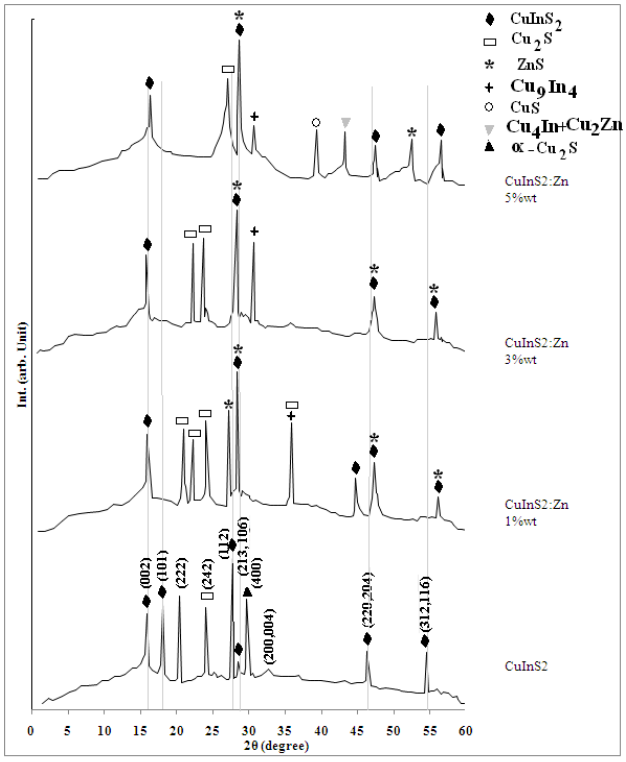

Fig.2. Shows the X-ray diffraction patterns of the undoped and doped films with Zn.

However, we can note a few peaks with lower intensities identified asCu_2 Zn+Cu_4In, CuS, Cu_2S and ZnS phases. The Presence of the phases is in general attributed to a sum of internal origins obeying the thermodynamics of solid solutions, to defect chemistry and the thermal gradient which plays an important role [21]. Indeed, the additional copper phase is mainly attributed to the higher mobility of Cu^+ and its migration toward the surface layers [22].

We can notes the overlap of zinc in most sites because of the similarity between the electronic-copper and zinc and the appearance of peaks at other locations a private compound ZnS and shift some peaks show the entry ions zinc to the crystal structure of the compound $CuInS_2$. This is consistent with what reported by Scherer and his group [23]. The short fall in the atoms of sulfur as a result of a link zinc- sulfur led to a surplus in the atoms of indium and copper, which resulted in formation and alloys Cu_4In and Cu9In4 as shown in Figure (2).

It has been established by Ueng and Hwang [24] that in studying the defect structure of zinc-doped $CuInS_2$, we have to consider the basic defect states that would be formed by zinc in $CuInS_2$ crystals. They show that the incorporation of zinc in $CuInS_2$ crystals can occur in three different ways, exclusively occupying the copper site to make a donor, occupying the sulfur site to make an acceptor and occupying the interstitial site to make a donor, and the donor ZnCu and Zn_i would be compensated by the acceptor ZnS. Consequently, it is probable that zinc in our case occupies the sulfur site to make an acceptor which can explain the origin of the *p*-type conductivity [25].

3.3. Optical properties

3.3.1. Absorption coefficient and optical band gaps

All the transmission spectra show interference pattern with moderate sharp fall of transmittance at the band edge, which is an indication of good crystallinity. The transmission of 1, 3 and 5 Zn % molecular weight doped $CuInS_2$ films are higher that of the non-doped .This indicates that an increase in Zn doping content from a critical Zn % molecular weight value has great effect on the transmission properties.

Therefore, for lower Zn concentrations there is an improvement in crystallinity through occupying the sulfur site by the zinc and the $CuInS_2$ structure is not affected. Consequently, there is an improvement in transmission in near infrared spectral range and probably the sulfur vacancy sites (samples undoped) increase the absorption. It is clear that the transmission in the near infrared region decreases from 70% to 35% for the higher Zn-incorporation. We consider that the introduced Zn with high amount compensates the sulfur vacancy sites after what the excess Zn atoms present an undesirable effect by decreasing the transmission in the near infrared spectral region. Although the detailed mechanism to explain the zinc effect in the decrease of the transmission is not clear yet [26].

The absorption coefficient (α) has been determined as a function of wavelength from measured reflectance R and transmittance T using the following equation [27], [28].

$$\alpha = 1/ d \ln [(1-R)^2 / T] \quad (1)$$

Where: d is the thickness of thin film, R and T are the reflection and the transmission respectively.

Fig. 3 shows the optical absorption coefficient, α as a function of the wavelength for $CuInS_2$ thin films prepared at different substrate temperatures. Higher absorption coefficient at higher substrate temperature.

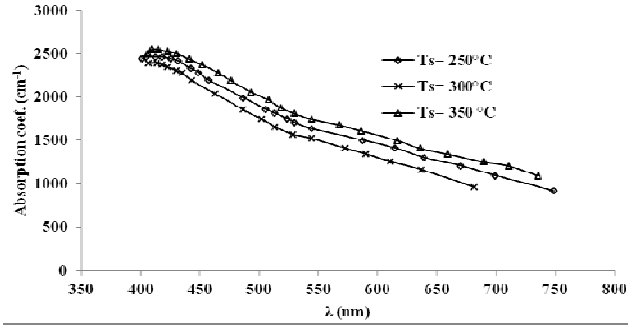

Fig.3.Optical absorption coefficients as a function of the wavelength for $CuInS_2$ thin films prepared at different substrate temperatures.

From the Fig. 4 we can see the values of absorption coefficient (α) increased when the film annealed in air to 200°C for 2.5 hours.

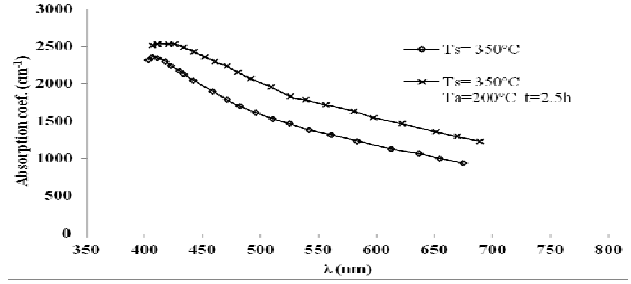

Fig.4. Values of absorption coefficient (α) for the film annealed in air to 200°C for 2.5 hours.

Fig. 5 shows the absorption coefficient versus the wavelength for the undoped and doped $CuInS_2$ thin films with 0 to 5 Zn % molecular weight. It can be seen that all the films have relatively high absorption coefficients.

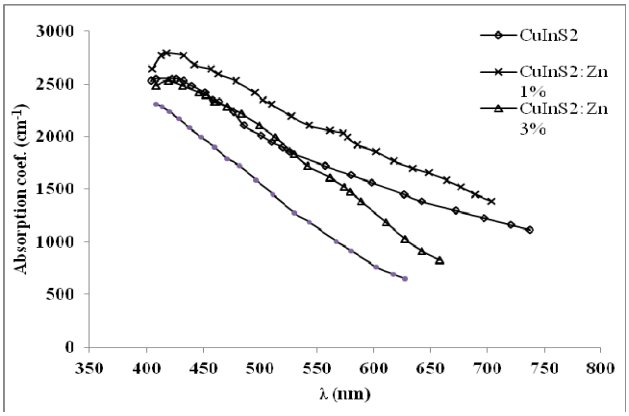

Fig. 5.Absorption coefficient versus the wavelength for the doped $CuInS_2$ thin films with (0 – 5) Zn % molecular weight.

Fig. 6 clearly shows an improvement in the optical performance of $CuInS_2$ films doped with 1 Zn % molecular weight with sharp fall of the absorption at the band edge compared to that of the un-doped or doped with other Zn content. This result is very important because we know that the spectral dependence of absorption coefficient affects the solar conversion efficiency [29].

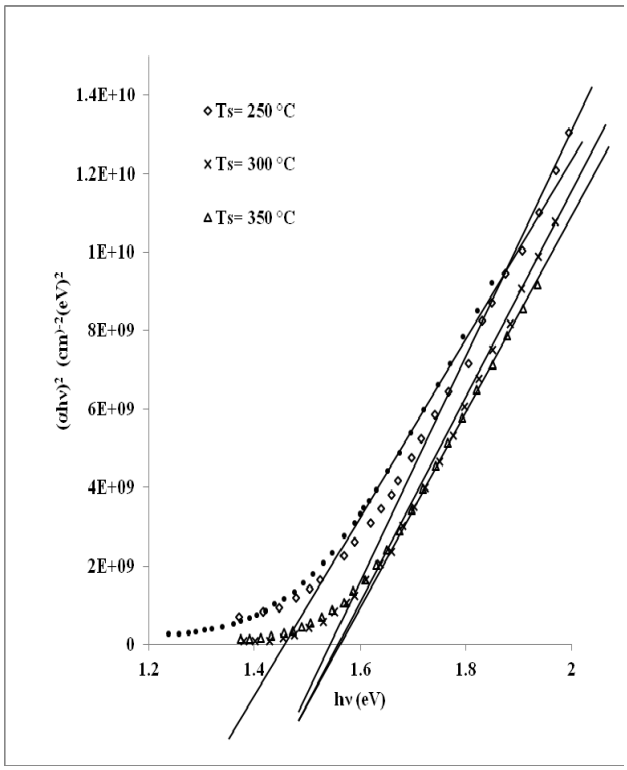

Fig.6. Shows a plot of (a hν)^2 against the photon energy as a function of different T_s.

In the high absorption region close to the beginning of band-to- band optical transmission, the absorption is characterized by the following relation [30, 31].

$$\alpha h\nu = A\,(h\nu - E_{opt})^{r} \quad (2)$$

Where A is a constant, E_{opt} is the optical gap and r is an integer number which characterizes the transition Process. The usual method for determining the values of E_{opt} involves plotting a graph of $(\boldsymbol{\alpha h\nu})^{r}$ **vs.** $h\nu$. An appropriate value of (r) is used to linearize the graph, the value of E_{opt} is given by the intercept on the hν axis and the constant A can be determined from the slope.

The best fit was found to be r = ½ which indicates that direct photon transition is involved.

Fig. 6 shows a plot of $(\boldsymbol{\alpha h\nu})^2$ against the photon energy **hν.** The band gap of the films is determined **by** the extrapolation of the curves. Its value in the films sprayed at ratios 1: 1: 4 is around 1.55 eV at 350^0C, which is more than the 1.53 eV energy gap value reported in the literature for $CuInS_2$ [5].

It is now well established that $CuInS_2$ is a direct gap semiconductor [32-34], with the band extrema located at the centre of the Brillouin. The direct band gap energy stabilizes between 1.55 eV and 1.95 eV with increasing the film Zinc concentration as shown in Fig. 7.

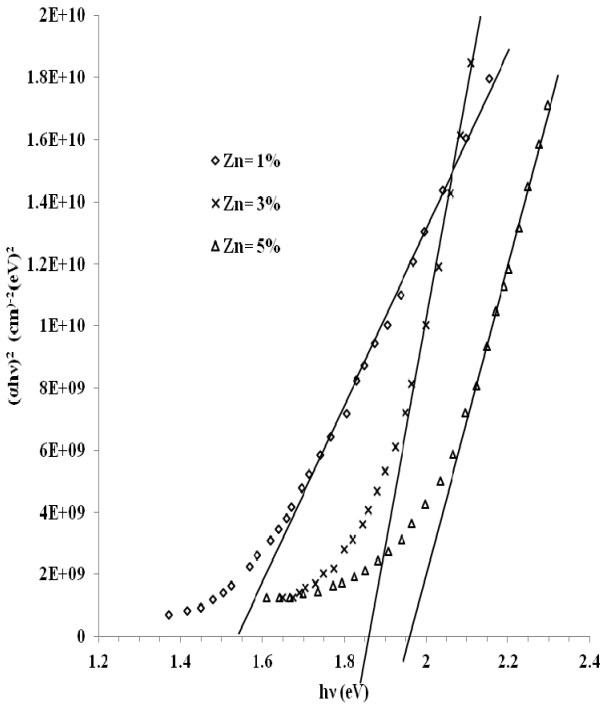

Fig.7. Shows a plot of (a hν)^2 against the photon energy as a function Zn doped films.

We attribute this difference to the presence of an amorphous component and possibly the structural defects, since it cannot be excluded that the polycrystallinity of the films influences the optical absorption behaviour and thus also the gap energy derived from the spectra. Also the amount of disorder in the material probably plays an important role in the optical band gap, since the XRD analysis indicated that for the higher Zn % molecular weight a deterioration of the structural properties was observed which give rise to defect states and thus induce smearing of absorption edge [35].

3.3.2. Refractive index

The refractive index was calculated using the following equation [36].

$$n= [4R/(R-1)^2 –K^2]^{1/2} - (R+1)/(R-1) \quad (3)$$

We observed from Figure (8) that the values of the refractive index of the prepared films are close together in the wavelength between (475-375) nm.

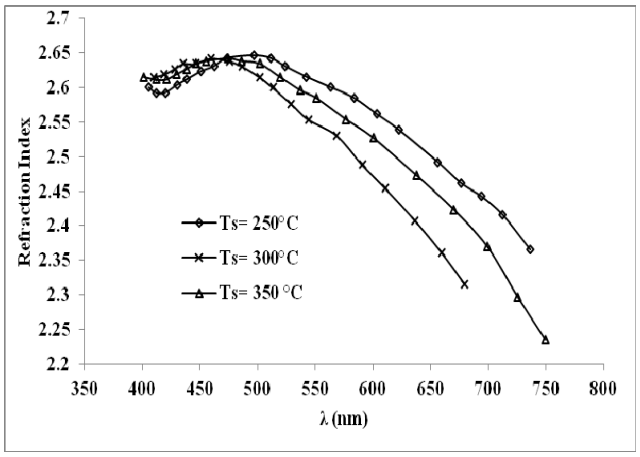

Fig. 8. Refractive index of the$CuInS_2$ films prepared at different substrate temperatures

The values of (n) at wavelength 550 nm were 2.61, 2.54 and 2.58 at substrate temperature 250,300 and 350 ^oC receptively.

When the films prepared at substrate temperature 350 ^oC and annealing to 200^oC for a period of 2.5 hours, it was observed that the values of the refractive index (n) was greater than that of deposited at T_s=350 ^oC (see Fig. 9).

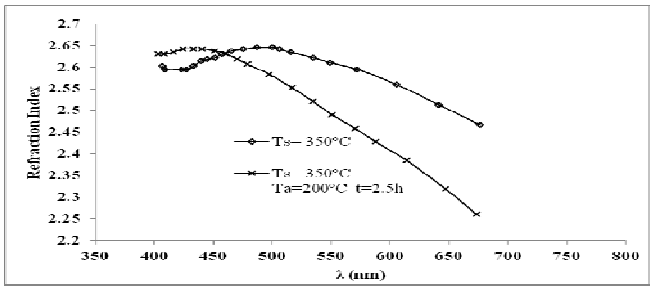

Fig. 9. Refractive index of $CuInS_2$ films prepared at T_s= 350 ^oC and annealing to 200^oC for 2.5 hours.

Access to the wavelength of 460 nm which reflected the situation with the note to increase the difference between them at greater the wavelength. The value of (n) at the wavelength of 550 nm was 2.492 as in Fig. (9).

Fig. (10) Shows the refractive index of $CuInS_2$ thin films doped with zinc ratios weighted (1, 3, 5) wt%.

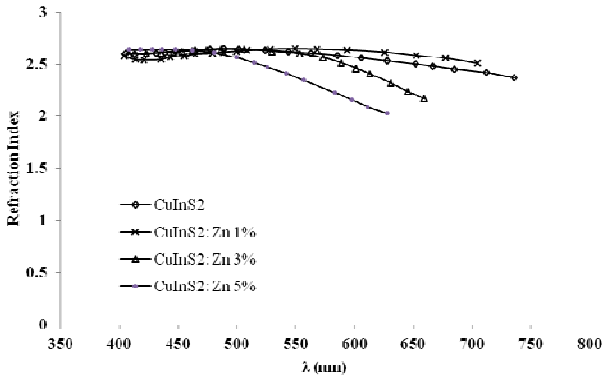

Fig. 10. Refractive index of $CuInS_2$ thin films doped with zinc ratios weighted (1, 3, 5) wt%.

We note that the increase in doping decreased the value of the refractive index, especially in the region (475-700) nm. The values of (n) at wavelength 550 nm were 2.37, 2.6 and 2.615 respectively, according to the percentage of doping.

3.3.3. Dielectric constant

The real and imaginary part of dielectric can be calculated from the following two equations [21]:

$$\varepsilon_1=n^2-k^2 \quad (4)$$

$$\varepsilon_2=2nk \quad (5)$$

Figure (11) shows the change in the real part of dielectric constant (ε_1) as a function of wavelength for $CuInS_2$ thin films deposited at different substrate temperatures.

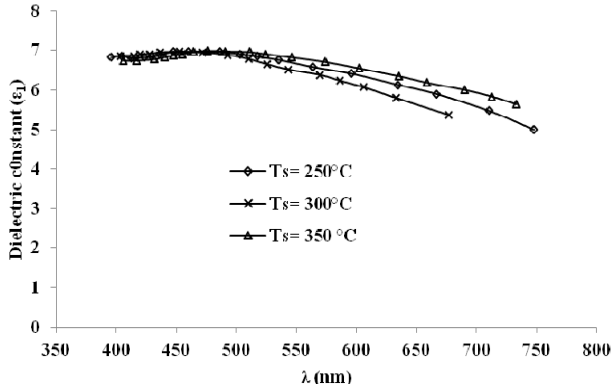

Fig.11. Values of (ε_1) as a function of wavelength for $CuInS_2$ thin films deposited at different T_s

We found that the values of (ε_1) at the wavelength of 550 nm were 6.49, 6.68, 6.81 at T_s=300, 250 and 350 ^oC respectively.

When $CuInS_2$ thin films doped with weight zinc (1, 3, and 5) wt%, we can see from Figure (12) that the values of (ε_1) decreases in the region of the visible with the increased rate of doping. The values of (ε_1) at a wavelength 550nm were depending on the rates of doping (1, 3, 5) at values of 5.65, 6.775 and 6.99 respectively.

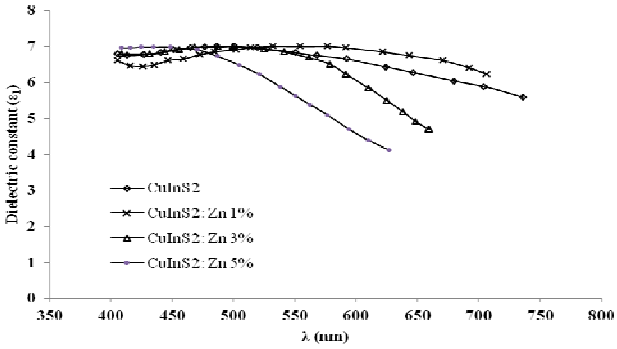

Fig. 12. Shows the value of (ε_1) as a function of wavelength at different doping

From Fig. (13) we can see the relation between the values of imaginary part of dielectric constant (ε_2) and wavelength. The values of (ε_2) were decreased when the substrate temperature increase from 250 ^oC to 300 ^oC, but increased when increasing the temperature to 350 ^oC and the values of (ε_2) of these films at wavelength 550nm with substrate temperatures basis (300,250,350) ^oC were (3.32, 3. 75 and 4.35)10^{-2} respectively.

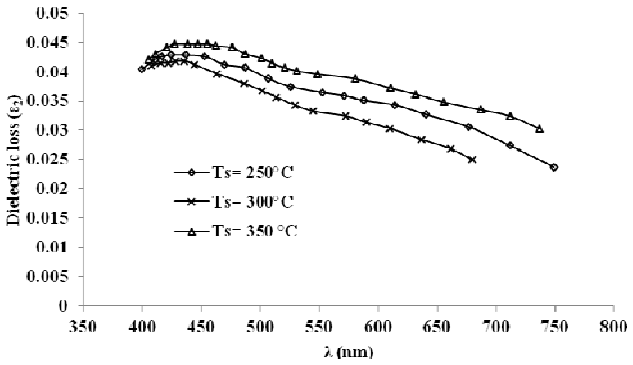

Fig.13. Values of (ε_2) as a function of wavelength at different substrate temperature

From Fig. 14 the values of (ε_2) decreases with increasing the doping and the values at the wavelength 550 nm were (2.31,3.875 and 4.525)10^{-2} with rates of doping (1,3,5)%, respectively.

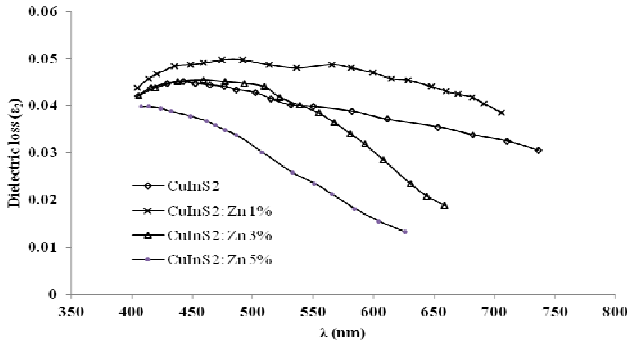

Fig. 14. The values of (ε_2) as a function of wavelength at different doping

4. Conclusions

The studies reported here show that it is possible to deposit CIS films using spray pyrolysis technique in ambient atmosphere using compressed air as carrier gas. Sprayed CIS films exhibit a chalcopyrite structure with a preferred orientation in the (112) direction. Structural, chemical composition and optical properties of sprayed films depend on the fabrication conditions, in particular on the substrate temperature and the Cu/In ratio in the starting solution.

It was found that the uniformity, growth rate and adhesion of the films depend strongly on the substrate temperature, spray rate and solution concentration.

The band gap of about 1.55 eV is in good agreement with the 1.53 eV energy values of CIS single crystal. The effect of Zn doping on the structural and optical properties of $CuInS_2$ thin films has been investigated. It was shown that Zn incorporation is possible and the control of Zn content is an important parameter to obtain Zn-doped $CuInS_2$ layers with high transmission. Moreover, up to 2 at % Zn the transmission decrease which indicates that an increase in doping content deteriorates the transmission properties. The absorption coefficients deduced from optical measurements are greater than $10^3 cm^{-1}$ in the range 400 nm. The direct band gap energy increased from 1.467 to 1.95 eV with increasing Zn % molecular weight. We attributed the higher values compared to that corresponding to the evaporated $CuInS_2$ thin films to the structural defects. The Zn-doped $CuInS_2$ thin films exhibit P-type conductivity

References

[1] P. S. Patil, Material Chemistry and Physics **59**, 185 (1999)
[2] K .Siemer, J. Klaer, I.Luck, J.Bruns, R.Klenk, D.Braunig, Sol. Energy Mater. Sol. Cells. **67,**159 (2001).
[3] I.Aksenov, K.Sato, J. Appl. Phys. **31**, 2352(1992).
[4] R.Scheer, K.Diesner, H.J.Lewerenz, Thin Solid Films **168,** 130(1995).
[5] J.L. Shay, J.H.Wernick, Ternary Chalcopyrite Semiconductors, Growth, Electronic Properties and Applications (Pergamon Press, New York, 1975).
[6] T.Hashimoto,S. Merdes, N.Takayama, H.Nakayama , H.Nakanishi, S.F.Chichibou , S.Ando, in: W. Palz, H. Ossenbrink, P. Helm (Eds.), 20th European Photovoltaic Solar Energy Conference, Proceedings of the International Conference, Barcelona, June 6 – 10, 1926(2005).
[7] M.Zribi, M.Kanzari , B.Rezig , in: W. Palz, H. Ossenbrink, P. Helm (Eds.), 20th European Photovoltaic Solar Energy Conference, Proceedings of the International Conference, Barcelona, June 6– 10, 1890(2005).
[8] J.S. NcNatt , J.E.Dickman , A.F.Hepp , C.V.Kelly , M.H.C.Jin , K.K.Banger , Conference Record of the 31st IEEE Photovoltaic Specialists Conference, Lake Buena vista, Florida, January 3 – 7, 375(2005).
[9] M.Zribi, M.Kanzari, B.Rezig, Jpn J. Appl. Phys. **29,** 203(2005).
[10] Y. Akaki, H.Matsuo, K.Yoshino, Phys. Stat. Sol. (c) **8,** 2597(2006).
[11] G.Brandt, A.Ranber, J.Schneider, Solid St.Commun. **12,** 481 (1983).
[12] S.D. Mittleman, R. Singh, Solid State Commun. **22**, 659 (1981).
[13] T.Yamamoto, H.K.Yoshida, Jpn. J. Appl. Phys. **35**, L1562 (1996).
[14] T.Yamamoto, V.Luck, R.Scheer, Appl. Surface Science **159 – 160**,350 (2000).
[15] M.Abaab, M.Kanzari, B.Rezig, M.Brunel, Solar Energy Materials & Solar Cells **59,** 299 (1999).
[16] T.Enzenhofer, T.Unold, R.Scheer, H.W.Schock, Physica Status Solidi A **203**, 2624 (2006)
[17] Horea Iustin NASCU, Violeta POPESCU, Leonardo Electronic J. of Practices and Techno. ISSN 1583-1078 Issue 4, January-June, 22 (2004).
[18] M.Ben Rabeh, M.Kanzari, B.Rezig, Thin Solid Films **515**, 5943 (2007).
[19] M. Sahal, B. Marí, M. Mollar, Thin Solid Films **517**, 2202 (2009).
[20] S. C. Ezugwu, F. I. Ezema, P. U. Asogwa, Chalcogenide Letters **7**, 396 (2010).
[21] S.C. Ezugwu, F.I. Ezema, R.U.Osuji, P.U. Asogwa, A.B.C. Ekwealor, B.A. Ezekoye, Optoelectron. Adv. Mater.-Rapid Comm. **3**,141 (2009).
[22] M. Kanzari, M. Abaab, B. Rezig, M. Brunel, Mater. Res. Bull. **32**, 1009 (19doped CuInS297).
[23] R. Scheer, K. Diesner, H.L. Lewerenz, Thin Solid Films **268**,130 (1995) .
[24] S.Schorr, M. Tovar, H. Bertin, 2009 Thin Solid Films **517**, 2508 (2009)
[25] H.Y. Ueng, H.L. Hwang, J. Phys. Chem. Solids **51**,11 (1990).
[26] S. Aksay, B.Altıokka, physica status solidi (c) **4**, 585 (2007).
[27] M. Ben Rabeh, M. Kanzari and B. Rezig**,** Acta Physica Polonica, **A115**, 699 (2009).

[28] D.E. Milovzorov, A.M. Ali, T. Inokuma, Y. Kurata, T. Suzuki, S. Hasegawa, Thin Solid Films **382**, 47 (2001).
[29] J. Tauc, R. Grigorovici, A. Vancu, Phys. Status Solidi **15**, 627 (1966).
[30] N.F. Mott, E.A. Davis, Philos. Mag. **22**, 903 (1970).
[31] E.A. Fagan, H. Fritzsche, J. Non-Crystal. Solids **2**, 80 (1970).
[32] K. Sedeek, M. Fadel, Thin Solid Films **229**, 223 (1993).
[33] B.Tell, J.L.Shay, H.M.Kasper, Phys.Rev. **B4**, 2463 (1971).
[34] H.Onnagawa, K.M. Miyashita, J.Appl.Phys. **23**, 965 (1985).
[35] N.N.Nishikawa, I.Aksenov, T.Sinzato, T.Sakamoto , K.Sato, Jpn.J.Appl.Phys, **34**, L975 (1995).
[36] N.F. Mott, E.A. Davis, Electronic Processes in Non—Crystalline Materials, Clarendon Press, Oxford 1971
[37] O.S. Heavens, Optical Properties of thin Solid Films, Butterworth's, London, 1950.

Corresponding author: mhsuhail@yahoo.com